Case Study of an Ice Sensor using Computational Fluid Dynamics, Measurements and Pictures - Boundary displacement

Marie Cecilie Pedersen
Dept. of Energy Technology
Aalborg University &
Vattenfall Vindkraft A/S
Kolding, Denmark
email: mcpe@et.aau.dk

Henrik Sørensen
Dept. of Energy Technology
Aalborg University
Aalborg, Denmark

Benjamin Martinez
Vattenfall Vindkraft A/S
Kolding, Denmark

Thomas Condra
Dept. of Energy Technology
Aalborg University
Aalborg, Denmark

***Abstract*—This paper presents an icing model developed using Computational Fluid Dynamics (CFD). One key part part of the model development is the surface boundary displacement due to the accumulated mass of ice. The paper presents the development of a boundary layer displacement method to be included in the CFD icing model using ANSYS-FLUENT.**

***Keywords:* ice accretion, surface boundary displacement, Computational Fluid Dynamics, dynamic-mesh, cold climate**

I. Introduction

Icing on wind turbines has been studied over the last 20 years and modelling of icing is a discipline, which has been approached by different methods and for different applications. Nevertheless, utility companies wish to improve and develop new and more precise turbine icing tools and production loss assessment models. The need for solving the energy and mass balance for droplets impinging on an object and to obtain the mass of accumulated ice over time is common for most of the tools. Within the wind power industry the model by Makkonen [1], originally developed for power line icing, has been widely used and is part of the iso standard iso-12494:2001 [2]. In recent work by Davis [3] the impact of icing on wind turbines was studied using Numerical Weather Prediction (WRF[1]) in combination with an icing model based on Makkonen's model [1], to forecast production losses due to icing. The original model [1] is empirically tuned for a cylinder but not a wind turbine. Thus, to improve on this fact [3] represents the turbine by a 1m long blade segment represented as a cylinder with a diameter based on the leading-edge radius of the given airfoil, and this showed promising results [4].

The power of the methodology by Davis [3] is the ability to study icing on an annual basis and the forecasting application provided by using the numerical weather models. However, details of a smaller time-scale from each individual icing event might be lost or not available. For future improvements of the methodology, a 3D CFD icing model specifically designed for wind turbines is put forward as a solution [3]. The methodology used by Vattenfall is similar to the overall approach seen in [3], but without any modifications to the Makkonen model. Similar to the conclusions from [3] experience have shown that changes to the ice model are essential to improve the overall production loss assessment methodology. Thus, this work aims to clarify whether a detailed CFD model can bring value into the current methodology for production loss assessment.

CFD models have met resistance in the wind power industry because of the computation time, the use of constant meteorological conditions and finally it has been questioned, if the accuracy gained from the micro-physics of a CFD simulations is necessary. In [5] an icing event of 17 hours was modelled using FENSAP-ICE based on data collected at a wind farm in Gaspé, Québec, Canada. The computational time was reduced by using a multi-shot approach of 34 steady-state simulations of 0.5 hours of icing, dividing the turbine blade into 9 stations and running the simulation in 2D. FENSAP-ICE is an commercial CFD code, which was originally developed for aircraft icing and is based on Messinger's model from 1953 [6]. The simulations were fed with observed values of temperature and wind speed and to obtain the power output a BEM-code was included. Another example of FENSAP-ICE being used for wind turbine application is seen in [7] and the [8], where performance degradation and power losses were studied and the possibilities of the design of an anti-icing system was proposed. The drawback of FENSAP-ICE is the strong link to the aircraft industry and that the model does not include shedding, which allows exaggerated ice horns to form [3]. Production loss assessment methods driven by numerical weather models [3] are typically fed with 1 hour based data. Such data can also be used in CFD simulations, as well as data of a much smaller time-scale. Furthermore, distributions of the Median Volumetric Diameter (MVD) can be included, which completely eliminates the issue of constant meteorological conditions.

A challenge when studying icing is the accessibility to observed and measured data. One problem is the reliability of the measurement equipment, as pointed out in [9]. Another is the complexity related to measuring and observing icing directly on the turbine itself, as seen at the TechnoCentre éolien, Quebec, Canada [10]. Thus, to circumvent the issue an ice sensor, installed at Vattenfall's Swedish wind farm, Stor-Rotliden, has been chosen as the foundation of the develop-

[1] Weather Research and Forecasting

ment of an CFD-based icing model for wind turbines. The ice sensor is combitec IceMonitor, which is a 0.5m long freely rotating cylinder with a diameter of 3cm. It is installed on a met mast together with other measurement equipment, as seen in Figure 1. From the CFD model development based on the IceMonitor, including testing and validation, the approach will be applicable to any geometry such as a turbine blade or a blade section. As the numerical platform of the study ANSYS-FLUENT has been used.

(a) (b)

Fig. 1. The IceMonitor to the left in the pictures at Stor-Rotliden wind farm with limited ice (a) and fully iced (b).

Other studies using ANSYS-FLUENT for icing applications are seen in [11] and [12]. In [11] the flow field around three different iced airfoils based on the airfoil (NACA 63-415) are simulated. The three geometries were obtained from experiments using in-fog icing conditions in a refrigerated wind tunnel. The k-ω SST turbulence model was used to study and compare numerical and experimental values of the lift, drag and pressure coefficients. A similar study was carried out in [12]. Another icing related study carried out using ANSYS-FLUENT is presented in [13], where the droplet collection efficiency (β) was calculated using an Eulerian frame, by employing the User-Defined-Scalar-Transport framework in ANSYS-FLUENT. In the Eulerian frame the collection efficiency was defined as:

$$\beta = \frac{\alpha_n(\mathbf{u} \cdot \mathbf{n})}{U_\infty} \tag{1}$$

where $\mathbf{n}$ is the unit surface normal vector, α_n is the normalised droplet volume fraction on the surface and U_∞ is the free-stream velocity. This approach, of calculating the collection efficiency, is equivalent to the approach by FENSAP-ICE presented in [14]. Common for the previous work carried out using ANSYS-FLUENT is:

- decoupling of the iced geometry obtained and studying the aerodynamic changes of the iced geometry
- decoupling of the impingement model and ice model with the geometry change of the iced object

However, this study aims to combine the entire process into a full icing model capable of:

1) Impingement model (multiphase flow and collection efficiency)
2) Ice model including runback
3) Generation of new geometry of iced object
4) Study of the aerodynamic changes and the ability to add a heat source for de-icing applications

This paper focuses on the generation of the new geometry of the iced object. This is an essential step, which has to be robust and able to handle any kind of ice accumulation on the surface. From a CFD point of view, two approaches are suitable for this purpose:

- variable porosity
- surface boundary displacement

If taking a look at fouling deposition modelled in various CFD-combustion applications, the underlying methodology is similar to the accumulation of ice. An example is the work seen by Knudsen [15], where a porosity model is developed in ANSYS-CFX to account for the geometry change due to ash deposition. Using porosity approach in CFD simply means prescribing a porosity to each cell and updating the porosity according to the accumulated mass. Thus, if the given cell is completely covered by mass of for example ash slag, the cell will be included as completely blocked in the CFD flow solution. In this way, the geometry change is taken into account. The advantage of this approach is that a complex mesh-update algorithm is avoided and the computational time is kept low. The drawback could be the need for a very fine mesh to account for smaller-scale geometry changes, which might be interesting to include in an ice accretion model.

The other way to account for the accumulated mass is to update the surface boundary mesh and generate a new iced geometry. In [16] a method to predict ice on an airfoil is presented using a 2D panel method and Messinger's model as the thermodynamic model. From the calculated mass of accumulated ice, the ice thickness is found as $h = \frac{\dot{m}_{ice}\Delta t}{\rho_{ice}\Delta s}$ (m), where ρ_{ice} is the ice density [16] [17]. The new surface is generated by first placing the new nodes at the corresponding thickness in a perpendicular direction to the old surface followed by connecting the nodes by average points between the nodes. To account for shape distortion and twisting of the grid, for example, glaze ice conditions, a smoothing algorithm is included, which can delete and renumber nodes. In [18] heat and mass transfer is studied with in improved roughness model for aircraft applications using a the 2D CIRAMIL code, which is a combination of a 2D potential flow solver and a thermodynamic solver. The panels are updated by using the bisection-method, which insures that the ice grows continuously in the normal direction to the surface. The panels are calculated based on the old nodes and the ice sections are limited by the bisection of angles with adjacent neighbouring panels. In FENSAP-ICE the mesh is updated similar to [16] by a surface displacement vector $\Delta h = \frac{\dot{m}_{ice}\Delta t}{\rho_{ice}}$, which is obtained from the ice accretion speed vector normal to the surface [19]. The ice accretion speed vector is used as an input to an Arbitrary Lagrangian-Eulerian (ALE) formulation to displace the surface in time [19] [20].

II. Method

The model is set-up in the environment of ANSYS-FLUENT following a preliminary modelling study [21]. The Euler-Euler multiphase model [22] is employed to express the two-phase droplet laden flow of air and super-cooled water droplets in combination with the k-ω SST turbulence model [11], assuming no coalescence or break-up of particles and no heat or mass transfer between the phases. As mentioned previously two methods are suitable for taking the accumulated mass of ice into account. In this study it was chosen to use the surface boundary displacement method. The surface boundary displacement are addressed by employing User Defined Functions. The entire method is illustrated by the flow-diagram in Figure 2.

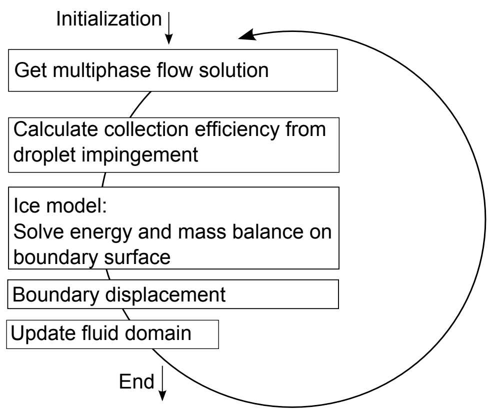

Fig. 2. Flow diagram of the modelling structure

A. Ice Model

In this study a simplified rime ice situation is modelled, since the surface boundary displacement is the main objective of the paper. Under rime ice accretion it is assumed, that all particles which hit the surface will freeze instantly and turn into ice. In fact, the complete model is based on a set of partial differential equations (PDEs), originally presented in [6]. The PDEs will be integrated in the model frame by the User-Defined-Scaler-Transport framework in ANSYS-FLUENT [23]. The mass of ice $\dot{m}_{ice}$ initiates the mesh update algorithm and is explained in the following section.

B. Boundary displacement

To insure a reliable and robust surface boundary displacement, the accumulated mass of ice has to be conserved, the ice growth is continuous and normal to surface and the displacement must be mesh independent. The surface boundary displacement is initialised by the Dynamic-mesh package by ANSYS-FLUENT [22], from where the DEFINE_GRID_MOTION macro is used, which is linked to an ANSYS-FLUENT node position algorithm. The macro is transient and by an iterative process the node points can be updated. The approach of this study is inspired by work using the ice height Δh_{ice} to displace the node points.

From the instantaneous accumulated mass of ice the mesh is updated by calculating a node displacement vector $\vec{v}_{n,i}$ giving an (x,y,z) coordinate of the new location of the node. The node displacement vector is obtained by a face-looping approach as follows:

1) Obtain face cell centre position displacement vector ($v_{f,i}$), see Equation 2
2) Relate/convert face cell centre position to new node positions
3) Move node point location by node displacement vector by an iterative mesh update process

$$v_{f,i} = \frac{\dot{m}_{ice}}{\rho_{ice}} \mathbf{n} \tag{2}$$

where, ρ_{ice} is the density of ice and $\mathbf{n}$ is the surface normal. Figure 3 illustrates the boundary displacement only based on the face centre displacement vectors. The shaded grey area is the area from each boundary cell, which is occupied by accumulated ice according to the face centre displacement vector. The red circle shows the inconsistent distribution of the accumulated mass of ice between the faces, which challenges the creation of the new surface boundary.

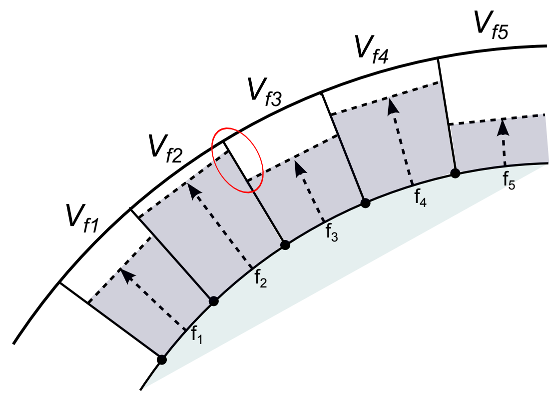

Fig. 3. Boundary displacement by face centre displacement vectors.

To circumvent the issue illustrated in Figure 3, corresponding node displacement vectors are found by liner interpolation, as illustrated in Figure 4. From this method, the total accumulated mass of ice in each boundary cell will be distributed evenly to created the new surface boundary of the object, illustrated by the dashed line.

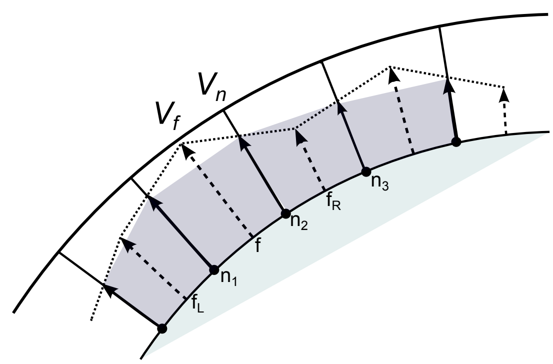

Fig. 4. Boundary displacement by converting face centre displacement vectors to node displacement vectors.

By the linear interpolation the contribution from the node neighbouring face, $\mathrm{f_L}$ and $\mathrm{f_R}$, to the node displacement vector is enabled. The nodes are updated according to the following expression:

$$p_{n,i}^{t+\Delta t} = p_{n,i}^{t} + v_{n,i}^{t} \Delta t \tag{3}$$

where $p_{n,i}$ is the current node positions, t is the current time and Δt the time step. The boundary layer displacement is fully transient, which means that the mesh is updated every time step.

III. RESULTS

Two 2D situations were studied, one with an angle of attack(aoa) of 0^o and one with an aoa of 16^o. The C-grid topology was used to generate the grid, which consist of an outer unstructered part and an inner structured part surrounding the cylinder, as seen in Figure 5.

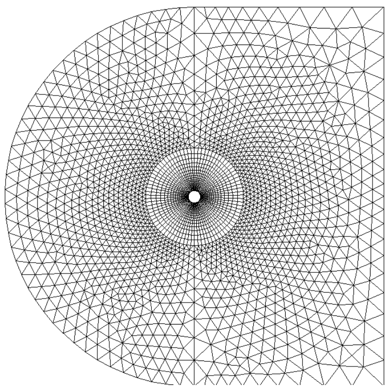

Fig. 5. Computational domain.

The conditions of the simulations are shown in Table I.

TABLE I. TEST CASE SETTINGS. * = NUMBER OF CELLS AT BOUNDARY

Parameter:		
Total no. cells	5013	mixed cells
BC cells*	82	no. cells
Time step size	0.01	(s)
Simulation time	15	(min)
aoa	0, 16	^{o}
U_∞	20	$\frac{m}{s}$
T_∞	-10	C^o
$\alpha_{d,\infty}$	$3.33 \cdot 10^{-7}$	$-$
LWC	0.3	$\frac{g}{m^3}$
MVD	10	μm

In the simulation it is assumed that $\dot{m}_{ice} \approx \dot{m}_{imp} = U_\infty LWC\beta$. This implies that all mass, which hit the object will freeze and accumulate on the boundary. The assumption is close to assuming rime ice accretion. The collection efficiency (β) at t = 0 min, for the two cases are seen in Figure 6. As expected the maximum collection is shifted to the left for the case of aoa = 16^o.

Figure 7 and Figure 8 shows the geometry change over 15 minutes of ice accretion, divided into intervals of 5 minutes. The ice growth is seen on the front of the cylinder around the stagnation point, which seems reasonable because of small MVD which results in the particles following the airflow and being deflecting around the object.

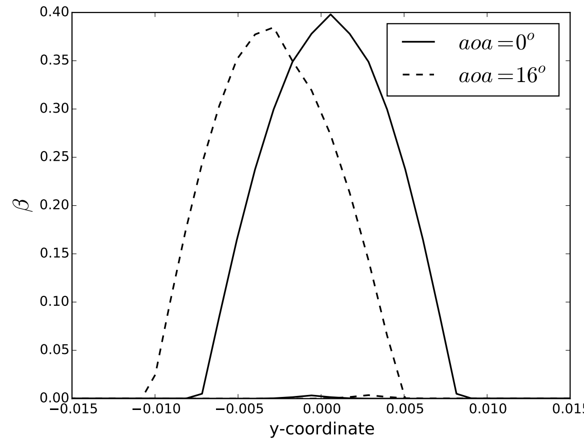

Fig. 6. Collection efficiency before ice accretion.

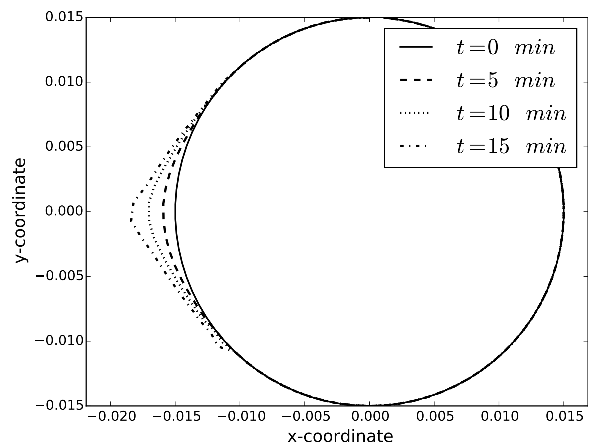

Fig. 7. Ice accretion shapes during 15 minutes of ice accretion at aoa of 0^o.

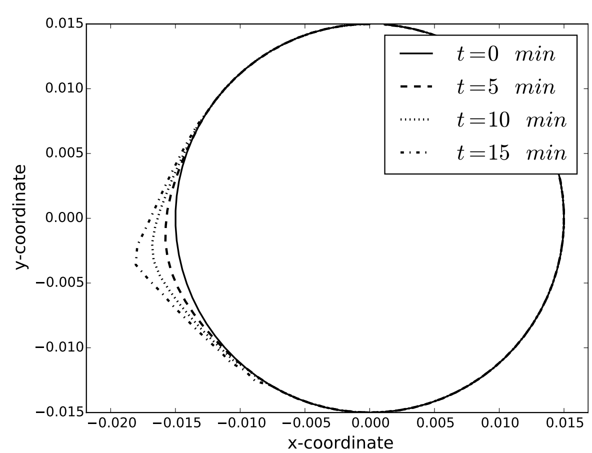

Fig. 8. Ice accretion shapes during 15 minutes of ice accretion at aoa of 16^o.

IV. Discussion and Conclusion

In this study it was found, that updating the mesh using the dynamic-mesh frame in ANSYS-FLUENT by applying a node displacement algorithm was feasible. A test case of 15 minutes of ice accretion was simulated successfully. To improve the mesh update a higher order discretisation scheme will be tested, such as the spline method. Furthermore, since the mesh update is fully transient it is time consuming especially for more dense mesh. Thus, for simulating longer icing events it is considered to let the model run in a so-called *quasi-steady* mode, similar to the 17 hours icing event in [24]. To improve on the ice model, a thermodynamic model will be included, which enables the study of glaze ice accretion and, for example, de-icing conditions.

Acknowledgement

Marie Cecilie Pedersen would like to thank Vattenfall R&D in Kolding and the Danish Agency for Science, Technology and Innovation for their financial support of the industrial PhD project.

References

[1] L. Makkonen, "Models for the Growth of Rime , Glaze , Icicles and Wet Snow on Structures," *Philosophical Transactions: Mathematical, Physical and Engineering Sciences*, vol. 358, no. 1776, pp. 2913–2939, 2000.

[2] T. S. S. Institute, "Athmospheric Icing on strutures, SS-ISO 12494," The Swedish Standards Institute, Tech. Rep., 2001, technical report.

[3] N. Davis, "Icing Impacts on Wind Energy Production," *PhD diss., Vestas Wind Systems A/S and The Technical University of Denmark, DTU Wind Energy*, 2014.

[4] N. Davis, A. N. Hahmann, N.-E. Clausen, and M. Žagar, "Forecast of Icing Events at a Wind Farm in Sweden," *Journal of Applied Meteorology and Climatology*, vol. 53, no. 2, pp. 262–281, 2014.

[5] D. Switchenko, W. G. Habashi, G. Baruzzi, and I. Ozcer, "FENSAP-ICE Simulation of Complex Wind Turbine Icing Events, and Comparison to Observed Performance Data," in *32nd ASME Wind Energy Symposium*, 2014.

[6] B. L. Messinger, "Equilibrium Temperature of an Unheated Icing Surface as a Function of Air Speed," *Journal of the Aeronautical Sciences (Institute of the Aeronautical Sciences)*, vol. 20, no. 1, pp. 29–42, 1953.

[7] T. Reid, G. Baruzzi, I. Ozcer, D. Switchenko, and W. Habashi, "FENSAP-ICE Simulation of Icing on Wind Turbine Blades, Part 1: Performance Degradation," in *51st AIAA Aerospace Sciences Meeting including the New Horizons Forum and Aerospace Exposition 07-10 January 2013, Grapevine (Dallas/Ft. Worth Region), Texas*, 2013.

[8] ——, "FENSAP-ICE Simulation of Icing on Wind Turbine Blades, Part 2: Ice Protection System Design," in *51st AIAA Aerospace Sciences Meeting including the New Horizons Forum and Aerospace Exposition*, 2013.

[9] H. Wickman, "Evaluation of Field Tests of Different Ice Measurement Methods for Wind Power," Uppsala University, Sweden, Tech. Rep., 2013, master Thesis.

[10] M. Wadham-Gagnon, "Wind Energy in Cold Climate," TechnoCentre éolien, Gaspe, Quebec, Canada, Tech. Rep., 2015, internal presentation at Vattenfall.

[11] F. Villalpando, M. Reggio, and A. Ilinca, "Numerical study of flow around iced wind turbine airfoil," *Engineering Applications of Computational Fluid Mechanics*, vol. 6, no. 1, pp. 39–45, 2012.

[12] X. Chi, B. Zhu, T. Shih, H. Addy, and Y. Choo, "CFD analysis of the aerodynamics of a business-jet airfoil with leading-edge ice accretion," *AIAA Paper*, vol. 560, 2004.

[13] S. Wirogo and S. Srirambhatla, "An Eulerian Method to Calculate the Collection Efficiency on Two and Three Dimensional Bodies," *AIAA paper*, vol. 1073, 2003.

[14] Y. Bourgault, Z. Boutanios, and W. G. Habashi, "Three-Dimensional Eulerian Approach to Droplet Impingement Simulation Using FENSAP-ICE, Part 1: Model, Algorithm, and Validation," *Journal of Aircraft*, vol. 37, no. 1, pp. 95–103, 2000.

[15] S. K. Kær, "Numerical Investigation of Deposit Formation in Straw-fired Boilers," *PhD diss., Aalborg University*, 2001.

[16] C. Son, S. Oh, and K. Yee, "Quantitative analysis of a two-dimensional ice accretion on airfoils," *Journal of Mechanical Science and Technology*, vol. 26, no. 4, pp. 1059–1071, 2012.

[17] Y. Cao, C. Ma, Q. Zhang, and J. Sheridan, "Numerical simulation of ice accretions on an aircraft wing," *Aerospace Science and Technology*, vol. 23, no. 1, pp. 296–304, 2012. [Online]. Available: http://dx.doi.org/10.1016/j.ast.2011.08.004

[18] G. Fortin, J.-L. Laforte, and A. Ilinca, "Heat and mass transfer during ice accretion on aircraft wings with an improved roughness model," *International Journal of Thermal Sciences*, vol. 45, no. 6, pp. 595–606, 2006.

[19] NTI, "User Manual FENSAP-ICE, Version 2012 release 1.1," Newmerical Technologies International, Montreal, Quebec, Canada, Tech. Rep., 2012, manual.

[20] W. Habashi, J. Dompierre, Y. Bourgault, M. Fortin, and M.-G. Vallet, "Certifiable computational fluid dynamics through mesh optimization," *AIAA journal*, vol. 36, no. 5, pp. 703–711, 1998.

[21] M. C. Pedersen and C. Yin, "Preliminary modelling study of ice accretion on wind turbines," *Energy Procedia*, 2014. [Online]. Available: http://dx.doi.org/10.1016/j.egypro.2014.11.1102

[22] ANSYS Inc, "ANSYS Fluent Theory Guide," ANSYS, Tech. Rep. Relaese 15.0, November 2013.

[23] Ansys Inc, "ANSYS Fluent UDF Manual," ANSYS, Tech. Rep. Relaese 15.0, November 2013.

[24] C. N. Aliaga, M. S. Aubé, G. S. Baruzzi, and W. G. Habashi, "FENSAP-ICE-UNSTEADY: Unified In-Flight Icing Simulation Methodology for Aircraft, Rotorcraft, and Jet Engines," *Journal of Aircraft*, vol. 48, no. 1, pp. 119–126, 2011.